COMPRESSION BEHAVIORS OF THICKNESS-REDUCED STEEL PIPES REPAIRED WITH UNDERWATER WELDS

X. CHEN[1*†], Y. KITANE[2], and Y. ITOH[3]

[1] *Department of Civil Engineering, Nagoya University, Japan*
[2] *Department of Civil Engineering, Nagoya University, Japan*
[3] *Department of Civil Engineering, Nagoya University, Japan*

ABSTRACT

Underwater welding is commonly used to repair corroded offshore steel structures. Corrosion-damaged portions are covered by welded patch plates. According to the current design manual, a thickness of patch plate and a weld length can be determined. However, different weld patterns can be designed to achieve the same required weld length. In order to examine the effectiveness of these different weld patterns, this paper first proposes a method to model underwater welds in the finite element analysis based on mechanical properties of fillet welds obtained from weld strength tests. The weld model was firstly validated against a theoretical shear stress distribution in a longitudinal fillet weld and then further validated against experimental results of thickness-reduced steel pipes repaired with welded patch plates under compression. The proposed model was then applied to thickness-reduced steel pipes repaired by welded patch plates with different weld patterns that have the minimum required weld length. Behaviors of these repaired pipes under a compressive load were examined with respect to stiffness, load-carrying capacity, load share of patch plates, and failure modes.

It was found that stiffness and load-carrying capacity of the thickness-reduced steel pipes under compression cannot be fully recovered by the welded patch plate repair when a patch plate thickness is the same as the thickness reduction of the damaged pipe. Among different weld patters, the one with four slits was found to show better performance.

Keywords: Underwater welding, repair, steel pipe pile, corrosion damage, finite element analysis.

1. INTRODUCTION

There are many offshore steel structures under severely corrosive environments all over the world, and many of them are in need of repair. Due to its high efficiency and cost effectiveness, patch plate repair by underwater welding is one of commonly used repair techniques. According to the current repair design manual in Japan (Coastal Development Institute of Technology 2009), a required

* Corresponding author: Email: chenxiao@civil.nagoya-u.ac.jp

† Presenter: Email: chenxiao@civil.nagoya-u.ac.jp

thickness of a patch plate and a required weld length can be determined when a corrosion-damaged structure is given. However, different welding patterns can be designed to provide the required weld length in the repair design. To find out the effect of welding patterns on compressive behaviors of repaired pipes, a comparative study was carried out in this paper by finite element (FE) analysis with a special attention paid to the modeling of underwater welds. The paper begins with a brief description and a result summary of weld strength tests, and then proposes a modeling method of weld in the FE analysis. The proposed weld model is then validated against analytical solutions and test results. By using the weld proposed model, three baseline repair designs for a thickness-reduced steel pipe are modeled. These repaired pipes are subjected to a compressive load in the FE analysis, and mechanical behaviors of the repaired pipes with different welding patterns are examined.

2. MODELING PROCEDURE OF MECHANICAL BEHAVIOR OF FILLET WELD

2.1. Weld strength test

Mechanical properties of underwater fillet welds were studied through a series of weld strength tests (Chen et al. 2010). The specimens were double strap joints welded by fillet welds. The specified weld leg length was 6 mm, and a length of one weld bead was 40 mm. Mechanical properties of fillet welds made on STK400 steel, structural steel tubes specified in JIS G3444, with SM400 patch plate, rolled steel plate for welded structure specified in JIS G3106, are summarized in Table 1.

Table 1: Mechanical properties of fillet welds*

Parameters	In-air		Underwater	
	Transverse	Longitudinal	Transverse	Longitudinal
Stiffness k_0 (kN/mm/mm)	31	14	41	14
Yielding stress σ_y (MPa)	433	193	443	265
Weld strength σ_w (MPa)	553	324	591	393
Ductility factor γ_m	0.15	0.32	0.10	0.16
Ductility factor γ_f	0.16	0.41	0.12	0.19

*Note: k_0 is the weld stiffness in loading direction per 1 mm's weld bead length; σ_y is determined by 0.2% offset value; σ_w is the maximum applied load divided by weld throat area; γ_m is the weld deformation at the maximum applied load divided by weld size; and γ_f is the weld deformation at weld fracture divided by weld size.

2.2. Modeling procedure

In this study, fillet welds are modeled as a number of connectors, as shown in Figure 1. Connector elements used are CONN3D2 for three-dimensional analyses in the general purpose finite element analysis software ABAQUS (Dassault Systèmes Simulia Corp 2008), and the connector type is "Cartesian" with three translational components, U_1, U_2, and U_3. Connector properties are defined in the form of an applied load-relative displacement curve for each component as shown in Figure 2, based on mechanical properties obtained in weld strength tests as following: (1) elastic response *OA* is characterized by linear stiffness $k=l_c \times k_0$, where l_c is the weld bead length that is represented by

one connector element; (2) plasticity onset point A is determined by k and the yielding load $P_y=\sigma_y\times l_c\times a$, where a is the size of weld throat; (3) Point B is the maximum load point determined by $P_m=\sigma_w\times l_c\times a$, and l_m is the corresponding displacement equal to $\gamma_m\times 1.414a$; (4) a power relation is assumed between Points A and B; (5) Point B is also referred to as the damage initiation point with a damage index d=0, and beyond this point, e.g. Point D, the stiffness and load-carrying capacity of the defined component in the connector is degraded from the undamaged state D', resulting in a softening post-peak response curve BDF, which is assumed to be a quarter of a sine curve; (6) Point F, referred to as the failure point with a damage index d=1, is determined by the fracture displacement $l_f=\gamma_f\times 1.414a$, where the stiffness and load-carrying capacity of the component in the connector become zero, and the connector element will be removed from the analysis.

It should be noted that three components of displacement, U_1, U_2, and U_3, in the connector are assumed to be mechanically independent until one of them reaches the failure. The force-displacement relationship in the direction of U_2 is determined by mechanical properties of longitudinal welds, and that of U_3 is determined by those of transverse welds. The force-displacement relationship of U_1, which is not available from weld strength tests, is assumed to be the same as that of U_3.

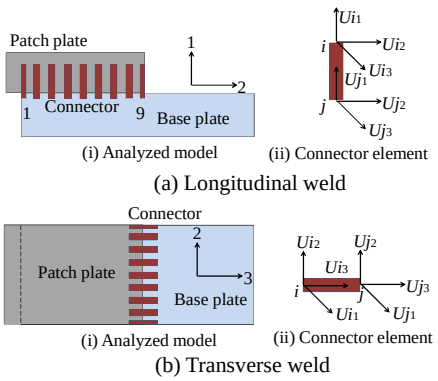

Figure 1: Weld model

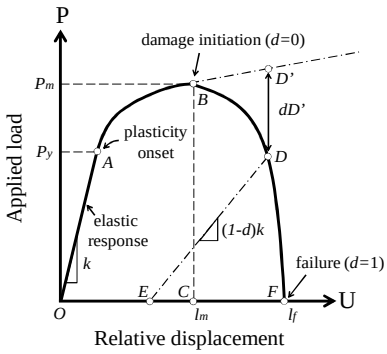

Figure 2: Connector behavior

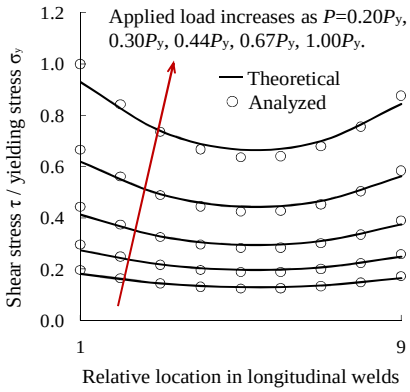

Figure 3: Shear stress distributions

3. MODEL VALIDATION

An initial validation is carried out for shear stress distribution in longitudinal fillet welds. Then, experimental results of two repaired pipes subjected to a compressive loading are used to further validate the model.

3.1. Stress distribution in longitudinal fillet welds

A theoretical distribution of shear stress in a longitudinal fillet weld in the elastic phase can be calculated by an existing formula (Suzuki 1982). A longitudinal fillet weld with a weld length of 40 mm is modeled by nine connector elements using a=4.2 mm. Two connector elements at the end of weld beads, as indicated as "1" and "9" in Figure 1(a)(i), are specified with l_c=2.5 mm, and the other seven connector elements are specified with l_c=5 mm. Comparisons of shear stress

distributions at different applied load levels are shown in Figure 3. It is found that analyzed distributions have good agreement with the theoretical ones along the weld bead despite a small overestimation of about 6% at the end of the weld bead in the relative location “1”.

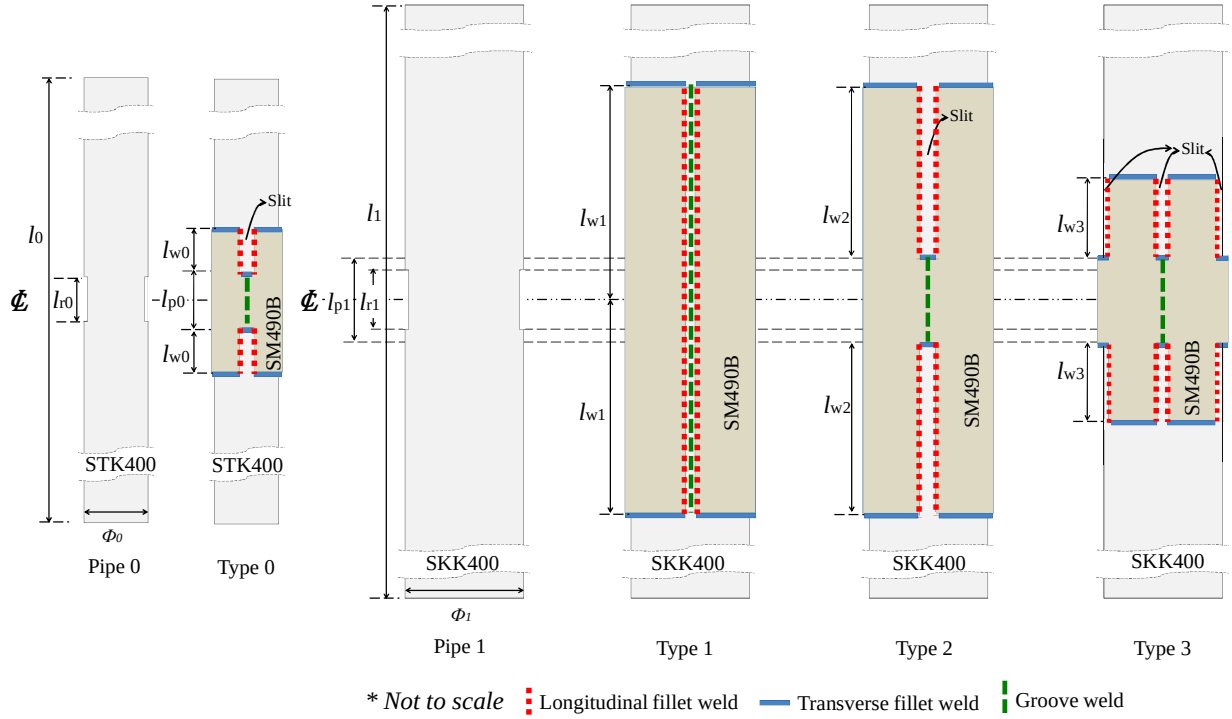

Figure 4: Examined pipes and repaired types

3.2. Validation against repaired pipe tests

Results from compressive tests of repaired pipes (Kitane et al. 2009) are used for further validation on the weld model. In this paper, two specimens, KA2C and KW2C, with welds made in air and underwater, respectively, are selected. These two specimens have the same dimensions, and are indicated as Type 0 in Figure 4 and Table 2. Fillet welds are modeled by connector elements, and groove welds which were used to joint two patch plates are modeled by shell elements with a thickness of 9 mm. The yielding stress of groove welds is estimated to be 600 MPa by assuming Vickers hardness of Hv200.

Table 2: FE model information (unit in mm)

	Pipe length	Thickness reduced length	Pipe diameter	Pipe thickness	Thickness reduction	Repair type	Length of each weld line	Groove weld length	No. of slits	Patch thickness
	l_i	l_{ri}	Φ_i	t_i	t_{ri}		l_{wj}	l_{gj}	n_j	t_{pj}
Pipe 0	1,500	150	216.7	12.6	6	Type 0	140	200	2	6
Pipe 1	5,600	500	500	12	6	Type 1	1,760	3,520	0	6
						Type 2	1,460	600	2	6
						Type 3	730	600	4	6

A quarter of specimen is modeled taking advantage of symmetry in the structural geometry as well as the loading condition. The size of weld throat used in the analysis is the measured value in the tests. Results from FEA are compared with those from the tests in Figure 5. Pipe shortening was measured for a length of 1,300 mm. Weld deformation was measured in the tests by clip gauges placed on transverse welds at the end of patch plates as indicated in Figure 6(b). Applied load P and pipe shortening δ are normalized by P_{y0}=2,815 kN, the theoretical yielding load of the intact pipe, and δ_{y0}=2.32 mm, the corresponding theoretical yield shortening, respectively.

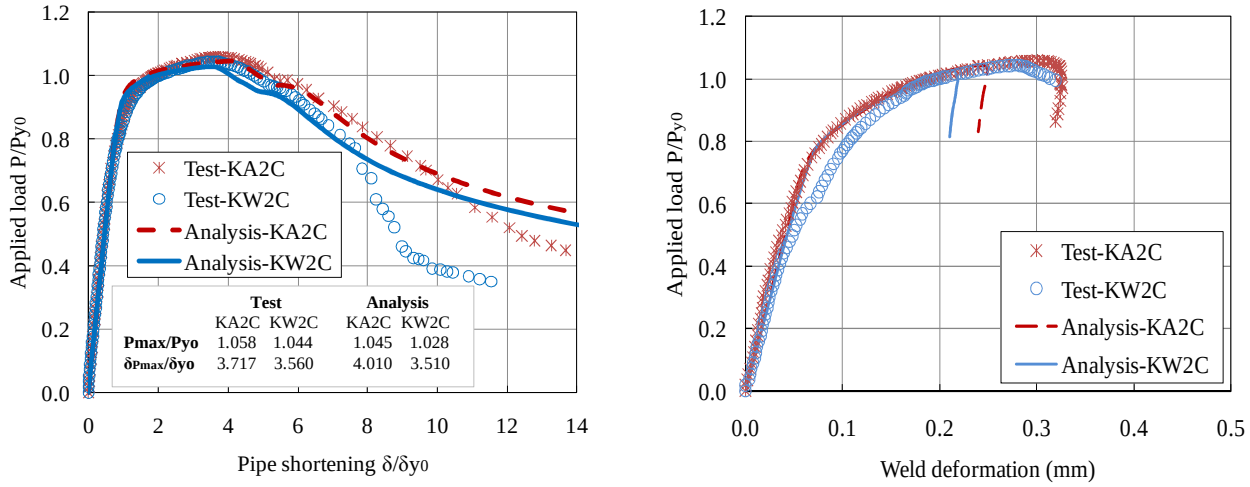

(a) Global responses of repaired pipes

(b) Local responses of weld deformation

Figure 5: Comparisons of validation tests on repaired pipe Type 0

It can be found that two analyzed models predict the global responses of two repaired pipes very well until pipe shortening δ/δ_{y0} is about 8 for KW2C and 10 for KA2C. A sudden decrease in the applied load in the test of KW2C at δ/δ_{y0}=8 was caused by the failure of groove welds, which are not considered to fail in the FE model. Overall transverse weld behaviors are predicted well, but there is an underestimation of the maximum weld deformation by about 20%.

A contour plot of equivalent plastic strain from the FE analysis at P/P_{y0}=0.8 in the post-peak region is used to examine failure modes of KW2C as shown in Figure 6(c). It is found that the test and the analysis both show that local buckling occurs at the thickness-reduced portion and that fillet welds fail at the corner of a slit in patch plates. An examination on the damage index *d* of welds in the analysis, as shown in Figure 7, shows that transverse weld elements #1 and #2 in the inner transverse weld line as indicated in Figure 6(d) reach their ultimate load first at δ/δ_{y0}=3.64. The longitudinal weld #1 adjacent to them then reaches the ultimate load at δ/δ_{y0}=4.33, followed by the longitudinal weld #2 at δ/δ_{y0}=5.95. A transverse weld bead on a patch plate which constitutes a re-entrant corner of a slit is referred to as an inner transverse weld in this paper. By comparing with δ_{pmax}, pipe shortening at P_{max}, this damage progress suggests that the repaired pipe, KW2C, reaches its maximum load when local buckling of the thickness-reduced portion of the pipe occurs at $\delta_{pmax}/\delta_{y0}$=3.51, and that buckling causes deformation of the pipe to increase. The increased relative deformation between the pipe and patch plates triggers the failure of the inner transverse weld, and

the adjacent longitudinal weld then becomes the damage-front. After that, weld failure progresses along the longitudinal weld bead, causing a total failure of the repaired pipe.

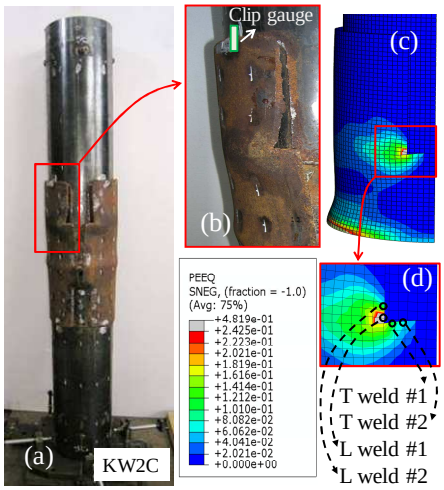

Figure 6: Comparison of failure modes

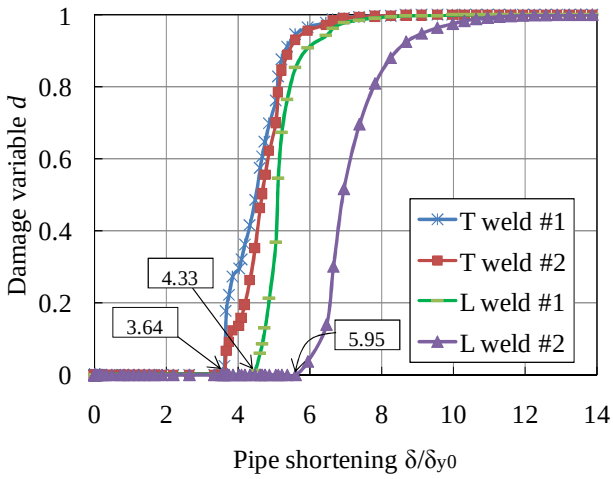

Figure 7: Damage progress of welds in KW2C

4. WELDING PATTERNS IN THE REPAIR DESIGN

In the repair design by welding patch plates, there can be different welding patterns as long as a total length of longitudinal welds meets the design requirements by the current repair manual. Moreover, transverse welds are not considered to provide any strength in the current design practice. In this study, three possible weld patterns are examined for repairing a thickness-reduced pipe pile. The pipe and its three repair designs are illustrated in Figure 4 as Pipe 1 and Type 1, 2, and 3. The size of pipe pile is selected from JIS A5525, and the grade is SKK400, which is a typical type of piles used in offshore structures in Japan. It should be noted that these three repair types are baseline designs where a thickness of patch plate is the same as the thickness reduction in the pipe, and the total length of longitudinal welds is just above the minimum required length according to the design manual. Their basic dimensions are listed in Table 2,

4.1. Examined weld patterns

Type 1 design uses two patch plates fillet-welded on a pipe pile, and two patch plates are welded together with groove welds. Longitudinal welds in this type are made not only on the intact pipe portion but also on the thickness-reduced portion. Groove welds overlap two longitudinal weld beads and are modeled as shell elements with a thickness of 3 mm and a yielding stress of 600 MPa. Type 2 design uses two slits in patch plates, and patch plates are fillet-welded to the pipe along slits. Two patch plates are groove-welded over the thickness-reduced portion. Type 3 design uses four slits in patch plates, and each longitudinal weld results in a half length of Type 2.

In Type 1, the length of longitudinal welds at the thickness-reduced portion is not counted in the design because the quality of longitudinal welds may not be as good as those at the intact portion. Therefore, Type 1 has longer longitudinal welds than Type 2 because of the extra length at the

thickness-reduced portion. However, all longitudinal welds of Type 1 are modeled in the same manner regardless of their locations, representing an upper bound condition.

Underwater fillet welds are modeled by the proposed weld model using a=4.2 mm and l_c=10 mm. To study the effect of transverse welds on compressive behaviors of repaired pipes, another set of these three models without transverse welds are also examined.

4.2. Results and discussions

Applied load and pipe shortening relationships of repaired pipes under compression are plotted in Figure 8. Applied load P and pipe shortening δ of a total pipe length are normalized by the theoretical yielding load of the intact pipe P_{y1}=6,660 kN and the corresponding theoretical yield shortening δ_{y1}=9.99 mm, respectively. Results are summarized in Table 3.

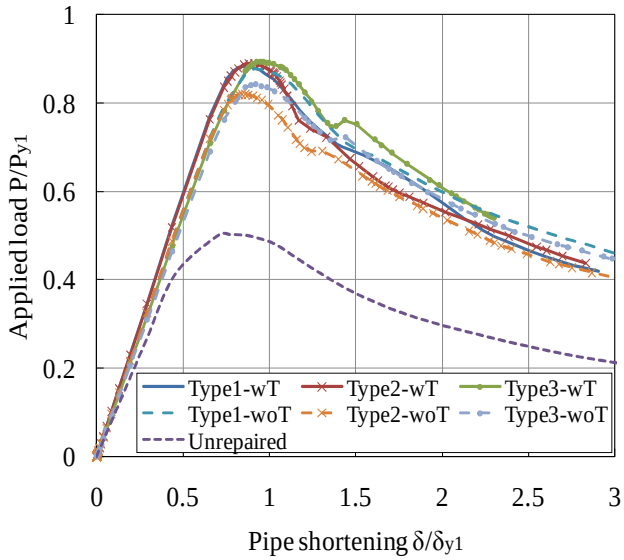

Figure 8: Global responses between different repaired types

Table 3: Summary of results*

Pipe	Stiffness K_r/K_{ry1}	Load-carrying capacity P_{max}/P_{y1}	Load share ratio of patch P_{patch}/P	Weld failure
Unrepaired	0.49	0.50	-	-
Type 1	0.82 (0.80)	0.88 (0.87)	0.44 (0.41)	None (None)
Type 2	0.79 (0.72)	0.88 (0.82)	0.44 (0.39)	Inner T and L (L)
Type 3	0.86 (0.81)	0.89 (0.84)	0.45 (0.42)	Inner T (L)

*Note: K_r is the axial stiffness of the thickness-reduced portion at $0.8P_{max}$. K_{ry1} (=7,465kN/mm) is the axial stiffness of intact Pipe 1 with a length of 500 mm. P_{max} is the maximum load. P_{y1} (=6,660kN) is the yielding load of the intact Pipe 1. P_{patch}/P is a load share ratio of patch plates at $0.8P_{max}$. Values in "( )" denote the cases without transverse welds.

It can be found that the stiffness of the thickness-reduced portion and load-carrying capacity of repaired pipes for all types cannot be fully recovered to those of an intact pipe, and the recovery rates range from 72% to 86% and from 82% to 89% for stiffness and load-carrying capacity,

respectively. The load share ratio of patch plates ranges from 0.39 to 0.45, meaning more load are carried by the thickness-reduced pipe piles rather than patch plates even though a wall thickness of the thickness-reduced portion is the same as the thickness of the patch plate.

Among three weld patterns, it is found that Type 3 shows a better performance in terms of strength and load-carrying capacity, while Type 2 appears to be the worst regardless of the existence of transverse welds. For the cases without transverse welds, it is obvious that both stiffness and load-carrying capacity are decreased for all types comparing to those with transverse welds. The reduction is found to be not so significant in Type 1 due to its continuous longitudinal weld beads along patch plates, which would decrease the relative deformation between the pipe and patch plates, and thus relieve shear stresses in longitudinal welds and eventually in transverse welds. For the same reason, there is no weld failure found in Type 1, although there are some in both Type 2 and Type 3. It deserves to note that if the quality of longitudinal welds at the thickness-reduced portion cannot be guaranteed, and if no longitudinal welds over the thickness-reduced portion can provide strength, behaviors of Type 1 under compression would be very similar to Type 2.

5. CONCLUSIONS

Using the proposed weld model, this paper studied the effect of different weld patterns on compressive behavior of a thickness-reduced pipe pile repaired with welded patch plates in the underwater environment by using the FE analysis. It was found that a baseline design where a thickness of patch plate is the same as the thickness reduction of the pipe cannot fully recover stiffness and load-carrying capacity under compression up to those of an intact pipe, and the recovery rates are about 80% and 86%, respectively. Among three examined designs, Type 3 with four slits in patch plates shows the best performance while Type 2 with two slits is the worst.

6. ACKNOWLEDGMENTS

This research was partially supported by The Japan Iron and Steel Federation and Nagoya University. The authors would like to acknowledge their supports. The first author also thanks the Chinese government for the scholarship during his doctoral study in Japan.

REFERENCES

Chen X, Kitane Y, and Itoh Y (2010). Mechanical properties of fillet weld joints by underwater wet welding in repairing corrosion-damaged offshore steel structures. Journal of Structural Engineering. 56(A). pp. 742-755.

Coastal Development Institute of Technology (2009). Port Steel Structure Corrosion-Prevention and Repair Manual, Coastal Development Institute of Technology, Japan (in Japanese).

Dassault Systèmes Simulia Corp (2008). ABAQUS/Standard user's manual, version 6.8.

Kitane Y, Itoh Y, Watanabe N, and Matsuoka K (2009). Compressive and flexural tests of thickness-reduced steel pipes repaired with patch plates using underwater wet welding. Journal of Structural Engineering. 55(A). pp. 889-902 (in Japanese).

Suzuki H.(1982). Recent Welding Engineering, Corona Publishing Co., Ltd., Tokyo, Japan (in Japanese).